Note: This copy is for your personal, non-commercial use only. To order presentation-ready copies for distribution to your colleagues or clients, contact us at www.rsna.org/rsnarights.

Assessment of Hepatic Steatosis in Patients Undergoing Liver Resection: Comparison of US, CT, T1-weighted Dual-Echo MR Imaging, and Point-resolved ^{1}H MR Spectroscopy[1]

Jochem R. van Werven, MD
Hendrik A. Marsman, MD
Aart J. Nederveen, PhD
Nico J. Smits, MD
Fiebo J. ten Kate, MD, PhD
Thomas M. van Gulik, MD, PhD
Jaap Stoker, MD, PhD

Purpose: To compare the diagnostic performance of ultrasonography (US), computed tomography (CT), T1-weighted dual-echo magnetic resonance (MR) imaging, and point-resolved proton (hydrogen 1[^{1}H]) MR spectroscopy in the assessment of hepatic steatosis in patients undergoing liver resection.

Materials and Methods: This prospective study was approved by the institutional review board, and patients gave written informed consent. US, CT, T1-weighted MR imaging, and ^{1}H MR spectroscopy were performed preoperatively in 46 patients. Imaging results were correlated (Spearman correlation coefficient) with histopathologic analysis of results of intraoperative liver biopsies. To assess differences between groups, one-way analysis of variance was used. Sensitivity and specificity were calculated for each imaging modality by using receiver operating characteristic curve analysis, with a histopathologic cut-off value of 5% macrovesicular steatosis. Differences in sensitivity and specificity were assessed by means of McNemar analysis.

Results: At histopathologic examination, 23 patients had no (0%–5%) macrovesicular steatosis, 11 had mild (5%–33%), nine had moderate (33%–66%), and three had severe (>66%). MR imaging and ^{1}H MR spectroscopic measurements of hepatic fat had stronger correlation with histopathologic steatosis assessment ($r = 0.85$, $P < .001$ and $r = 0.86$, $P < .001$, respectively) than did US ($r = 0.66$, $P < .001$) and CT ($r = -0.55$, $P < .001$). Only T1-weighted MR imaging and ^{1}H MR spectroscopy showed differences across steatosis grades: none versus mild ($P = .001$ for both), mild versus moderate ($P < .001$ for both), and moderate versus severe ($P = .04$ and .01, respectively). Sensitivity of US, CT, T1-weighted MR imaging, and ^{1}H MR spectroscopy was 65% (13 of 20), 74% (17 of 23), 90% (19 of 21), and 91% (21 of 23), respectively, and specificity was 77% (17 of 23), 70% (14 of 20), 91% (20 of 22), and 87% (20 of 23), respectively.

Conclusion: In contrast to US and CT, T1-weighted MR imaging and ^{1}H MR spectroscopy strongly correlate with histopathologic steatosis assessment and are able to demonstrate differences across steatosis grades. T1-weighted dual-echo MR imaging and ^{1}H MR spectroscopy had the best diagnostic accuracy in depicting hepatic steatosis.

©RSNA, 2010

[1] From the Departments of Radiology (J.R.v.W., A.J.N., N.J.S., J.S.), Surgery (H.A.M., T.M.v.G.), and Pathology (F.J.t.K.), Academic Medical Center, University of Amsterdam, Meibergdreef 9 1105 AZ Amsterdam, the Netherlands. From the 2009 RSNA Annual Meeting. Received October 2, 2009; revision requested November 11; revision received January 7, 2010; accepted January 13; final version accepted January 20. Supported by the Nuts Ohra Foundation. **Address correspondence to** J.R.v.W. (e-mail: *j.r.vanwerven@amc.uva.nl*).

©RSNA, 2010

Nonalcoholic fatty liver disease is characterized by lipid accumulation in the liver and affects up to 30% of the Western population (1). It is associated with obesity, diabetes, and metabolic syndrome (2). The prevalence of nonalcoholic fatty liver disease is expected to increase due to the current obesity epidemic (3). Nonalcoholic fatty liver disease represents a disease spectrum that ranges from simple hepatic steatosis to steatohepatitis to fibrosis and cirrhosis. Ultimately this can lead to end-stage liver failure, with subsequent need for a liver transplant, or the development of hepatocellular carcinomas (4). Nonalcoholic fatty liver disease has also been recognized as a risk factor in patients undergoing liver surgery (5,6).

Currently, the reference standard for hepatic steatosis assessment is histopathologic analysis of a liver biopsy (7). This is an invasive procedure with the potential of complications. Liver biopsy is also prone to sampling error and interobserver variability (8,9). Furthermore, the determination is semiquantitative. Consequently, there is a need for noninvasive diagnostic tools for the detection and quantification of steatosis and monitoring.

To date, several imaging techniques are used to detect hepatic steatosis: ultrasonography (US), computed tomography (CT), magnetic resonance (MR) imaging, and proton (hydrogen 1[^{1}H]) MR spectroscopy (10). US is a widely available and low-cost technique. However, US is not quantitative, is inaccurate in obese patients (11), and is not useful in detection of low levels of steatosis (12,13). CT is accurate in a semiquantitative diagnosis of macrovesicular steatosis of 30% or greater (14), but its use for monitoring treatment response is somewhat limited due to exposure to ionizing radiation. MR imaging is performed by using gradient-echo chemical shift imaging (Dixon method), either as a readily available T1-weighted dual echo, triple echo, multiecho, or multiinterference (15,16). ^{1}H MR spectroscopy is considered the most sensitive noninvasive modality for the detection of hepatic fat (17) and has shown good reproducibility (18). However, in most centers, ^{1}H MR spectroscopy remains largely a research tool.

Authors of some studies have compared imaging modalities to assess steatosis, and findings showed strong significant correlation between MR imaging and ^{1}H MR spectroscopy (r = 0.96–0.99) and between ^{1}H MR spectroscopy and CT (r = 0.83). However, these results were not compared with liver biopsy results (19–22). Other studies however did compare imaging modalities with histopathologc studies and showed substantial variation in correlations (23–28).

To our knowledge, no head-to-head comparative study of US, CT, T1-weighted dual-echo MR imaging, and ^{1}H MR spectroscopy with use of readily available methods has been performed and compared with the reference standard histopathologic analysis. Therefore, the purpose of this study was to compare the diagnostic performance of US, CT, T1-weighted dual-echo MR imaging, and point-resolved ^{1}H MR spectroscopy in the assessment of hepatic steatosis in patients undergoing liver resection.

Advances in Knowledge

- T1-weighted dual-echo MR imaging and ^{1}H MR spectroscopy strongly correlate with histopathologic steatosis assessment (r = 0.85 and 0.86, respectively).
- T1-weighted dual-echo MR imaging and ^{1}H MR spectroscopy had the best diagnostic accuracy (91% [39 of 43] and 89% [41 of 46], respectively) in detecting hepatic steatosis, with acceptable sensitivity (90% [19 of 21] and 91% [21 of 23], respectively) and specificity (91% [20 of 22] and 87% [20 of 23], respectively).
- Compared with US (accuracy, 71% [30 of 42]; sensitivity, 65% [13 of 20]; specificity, 77% [17 of 22]) and CT (accuracy, 72% [31 of 43]; sensitivity, 74% [17 of 23]; specificity, 70% [14 of 20]), T1-weighted dual-echo MR imaging and ^{1}H MR spectroscopy are superior in assessment of hepatic steatosis and grading steatosis.

Implication for Patient Care

- T1-weighted dual-echo MR imaging and ^{1}H MR spectroscopy are the preferred imaging techniques for noninvasive assessment of hepatic steatosis.

Materials and Methods

A research grant was received from the Nuts Ohra Foundation (Amsterdam, the Netherlands). The Nuts Ohra Foundation was not involved in designing and conducting this study, did not have access to the data, and was not involved in data analysis or preparation of this manuscript.

Study Design and Patients

This prospective study was approved by the institutional review board. All patients gave written informed consent. No conflicts of interested were noted.

From November 2007 through March 2009, all patients 18 years of age and older who were scheduled to undergo a liver resection were consecutively invited to participate in this study. The main indications for liver resection were colorectal metastases in 48% (22 of 46) of patients, adenoma in 15%

Published online
10.1148/radiol.10091790

Radiology 2010; 256:159–168

Abbreviations:
AUC = area under the ROC curve
ROC = receiver operating characteristic
ROI = region of interest

Author contributions:
Guarantors of integrity of entire study, J.R.v.W., H.A.M., A.J.N., F.J.t.K., T.M.v.G., J.S.; study concepts/study design or data acquisition or data analysis/interpretation, all authors; manuscript drafting or manuscript revision for important intellectual content, all authors; approval of final version of submitted manuscript, all authors; literature research, J.R.v.W., H.A.M.; clinical studies, J.R.v.W., H.A.M., A.J.N., F.J.t.K., T.M.v.G., J.S.; experimental studies, H.A.M., T.M.v.G.; statistical analysis, J.R.v.W., H.A.M., A.J.N.; and manuscript editing, J.R.v.W., H.A.M., A.J.N., T.M.v.G., J.S.

Authors stated no financial relationship to disclose.

(seven of 46), and cholangiocarcinoma in 13% (six of 46) (Table 1). Demographic characteristics and body mass index were recorded. Exclusion criteria were pregnancy, acute liver resection, and MR contraindications. No patients were excluded. Patients underwent preoperative abdominal US, CT, T1-weighted MR imaging, and ^{1}H MR spectroscopy for the detection of hepatic steatosis.

Imaging Techniques

US examination.—US was performed with an iU22 (Philips Healthcare, Best, the Netherlands) device by using a 2–5-MHz probe or an Elegra (Siemens Healthcare, Erlangen, Germany) device by using a 3.5-MHz probe. An experienced abdominal radiologist (N.J.S.), with more than 25 years of liver US experience, blinded to other study results scored the degree of steatosis. The reader did not undergo a training session. Experience does not automatically imply accurate grading of liver fat. However, the observer routinely grades liver steatosis to assess its severity. On the basis of increasing echogenicity of the liver parenchyma compared with that of the right kidney and decreased visualization of the diaphragm and intrahepatic vessel borders, steatosis in each patient was graded as none (normal US liver structure), mild (slight increase of echogenicity, normal visualization), moderate (diffuse increase of echogenicity, slight impaired visualization), or severe (marked increase of echogenicity, poor or no visualization) (29,30).

CT examination.—Unenhanced CT examinations were performed with a Brilliance (Philips Healthcare) 64-section scanner and the following parameters; 120 kV, 200 mAs with dose modulation, collimation of 64 × 0.625, section thickness of 3 mm, and an increment of 3 mm. Data were processed by a research fellow (J.R.v.W.) under direct supervision of an experienced abdominal radiologist (J.S., 15 years of experience), blinded to the study results. On three CT sections, four regions of interest (ROIs) were drawn in the liver (12 ROIs total) evenly distributed in the hepatic parenchyma, avoiding tumor lesions and biliary, vascular, and extrahepatic structures. ROI size was 5 cm^2 and section selection was based on the anatomy of the liver, usually in the middle section of the liver (avoiding the cranial and caudal part of the liver). Hepatic fat content was measured by using mean liver attenuation of all ROIs in the liver (31). To assess the possible effect of heterogeneity of fat in the liver on the diagnostic accuracy, we compared diagnostic performance of CT in the left liver lobe to that in the right liver lobe and within the right lobe.

T1-weighted dual-echo MR imaging.—A 3.0-T Intera MR imager (Philips Healthcare) with a six-channel torso coil was used to obtain MR and ^{1}H MR spectroscopic images during the same procedure (imaging time, 30 minutes). T1-weighted dual gradient-echo sequence parameters were as follows: repetition time msec/echo time msec, 150/3.5 (opposed phase), 6.9 (in phase); flip angle, 75°; section thickness, 7.0 mm; 18 sections; field of view, 400 × 280 mm; breath hold, 15 seconds. As was performed for CT, at three different sections, four ROIs were drawn evenly distributed in the liver parenchyma (12 ROIs total), avoiding other anatomic structures. ROI location on CT and T1-weighted dual-echo MR images was visually chosen as accurately as possible on the same position in the liver. The mean signal intensity values of all ROIs were determined at the same locations for in-phase and opposed-phase MR images. Mean fat fraction was calculated by using the following equation (32): $SI_{IP} - SI_{OP}/2SI_{IP,}$ where SI_{IP} and SI_{OP} are the mean liver signal intensity of all ROIs on in-phase and opposed-phase images, respectively. Data were processed with ImageJ software (33) by a research fellow (J.R.v.W.) under direct supervision of an experienced MR physicist (A.J.N., 5 years of experience), blinded to the study results. Again, heterogeneity was assessed by comparing diagnostic performance of T1-weighted dual-echo MR imaging in the left liver lobe to that in the right liver lobe and within the right lobe.

^{1}H MR spectroscopy.—A 20 × 20 × 20-mm voxel was positioned in the right liver lobe. The voxel was placed distant from the tumorous liver tissue. Spectra were acquired by using first-order iterative shimming and a point-resolved spectroscopy sequence (2000/35, 64 acquisitions). The water and fat resonance peaks, located at 4.65 and 1.3 ppm, were fitted by using a spectroscopic analysis package (jMRUI; A. van den Boogaart, Catholic University, Leuven, Belgium) (34), and relative fat content was expressed as a ratio of the fat peak area over the cumulative water and fat peak areas (1.3 ppm/[1.3 ppm + 4.65ppm]). Calculated peak areas of water and fat were corrected for T2 relaxation ($T2_{water}$ = 34 msec, $T2_{fat}$ = 68 msec) (35), and the percentage hepatic fat content was calculated according to Szczepaniak et al (17).

Liver Tissue Sampling

During surgery, a large wedge biopsy specimen (20 × 20 × 20-mm) from the part of the liver to be resected was retrieved, distant from the liver masses and liver capsule. Liver tissue samples were fixed in 10% buffered formalin for 24 hours, and 4-μm-thick sections were stained with hematoxylin-eosin. No separate staining for iron was performed.

Table 1

Indications for Liver Resection

Indication for Liver Resection	No. of Patients
Colorectal metastases	22 (47.8)
Adenoma	7 (15.1)
Cholangiocarcinoma	6 (13.0)
Focal nodular hyperplasia	2 (4.3)
Hepatocellular carcinoma	1 (2.2)
Hemangioma	1 (2.2)
Gallbladder carcinoma	1 (2.2)
Mamma carcinoma metastasis	1 (2.2)
Melanoma metastasis	1 (2.2)
Metastasis of neuroendocrine tumor	1 (2.2)
Choledochal cyst	1 (2.2)
Stenosis ductus hepaticus	1 (2.2)
Intrahepatic bile duct stones	1 (2.2)
Total	46 (100)

Note.—Data in parentheses are percentages.

Fibrosis and inflammation were not assessed.

Histopathologic Steatosis Assessment

An experienced hepatopathologist (F.J.t.K., 30 years of experience), blinded to study results, evaluated the liver biopsy samples for histopathologic grading of hepatic steatosis. Macrovesicular steatosis was assessed as the percentage of hepatocytes in the microscopic field containing a lipid vacuole larger than the diameter of the nucleus and displacing the nucleus. Percentage of macrovesicular steatosis was graded as none (0%–5%), mild (5%–33%), moderate (33%–66%), and severe (>66%) (36). Microvesicular steatosis was assessed as the percentage of hepatocytes in the microscopic field containing numerous small vesicles not displacing the nucleus.

Statistical Analysis

Correlations between results of imaging modalities and histopathologic results (percentage macrovesicular steatosis) were assessed by using Spearman correlation coefficient. We also studied correlations specifically in patients with proved hepatic steatosis to investigate the influence of the findings in patients without hepatic steatosis on the overall correlations. We did not evaluate intraobserver agreement for the imaging techniques and the reference standard. Differences between groups were assessed with one-way analysis of variance by using post hoc Bonferroni correction. We also performed receiver operating characteristic (ROC) curve analysis to determine the best cut-off values for US, CT, T1-weighted dual-echo MR imaging, and ^{1}H MR spectroscopy to predict hepatic steatosis. To assess test accuracy, we evaluated the area under the ROC curve (AUC). The best cut-off value was determined while balancing the best sensitivity with the lowest false-positive rate. Performance statistics (total accuracy, sensitivity, specificity, positive predictive value, negative predicative value, and likelihood ratio) with 95% confidence intervals were evaluated by means of the best cut-off value to assess hepatic steatosis for the four imaging techniques. The likelihood ratio is the likelihood that a test result would be expected in a patient with the target disorder compared with the likelihood that the same test result would be expected in a patient without the target disorder. A likelihood ratio greater than 10 and less than 0.1 imply strong effects, whereas a likelihood ratio of 1 implies no effect. Differences in sensitivity and specificity were assessed by using a McNemar test. For Bonferroni corrections, the level of significance was corrected for the number of comparisons (P value: .05/6 = .0083). For all other statistical analysis a P value < .05 was considered to indicate as significant difference. All statistical analyses were performed by using software (SPSS version 16.0; SPSS, Chicago, Ill).

Results

Patients

The study included 46 patients, 25 (54%) men and 21 (46%) women, with a mean age of 58.7 years (range, 27–76 years) (Fig 1). The mean age for men was 65.2 years (range, 48–76 years) and that for women was 50.9 years (range, 27–76 years). The mean body mass index was 27.1 kg/m^2 (range, 20.2–40.6 kg/m^2), with 26.2 kg/m^2 (range, 20.8–34.0 kg/m^2) in men and 28 kg/m^2 (range, 20.2–40.6 kg/m^2) in women. Considering a mean body mass between 20 and 25 kg/m^2 to be normal, 41% (19 of 46) of the patients had normal weight and 59% (27 of 46) were overweight. US, T1-weighted dual-echo MR imaging, and ^{1}H MR spectroscopy were all performed within 2 weeks prior to liver resection. CT was performed within 3 months prior to surgery. Four US and three CT examinations were not performed because of logistical reasons, and three dual-echo MR imaging examinations were not performed because of technical failure.

Histologic Reference Standard

At histopathologic examination, 23 patients had none, 11 had mild, nine had moderate, and three had severe macrovesicular steatosis. The prevalence of hepatic steatosis in this study population was 50% (23 of 46 patients had macrovesicular steatosis > 5% at histopathologic analysis). Mean macrovesicular steatosis was 16.1% (range, 0%–80%), and mean microvesicular steatosis was 6.5% (range, 0%–25%). Correlation between macro- and microvesicular steatosis was significant (r = 0.67, P < .001).

Correlations

Table 2 shows correlation coefficients of the imaging techniques versus histopathologic examination. Figure 2 shows correlations graphically. A moderate correlation was found between US and macrovesicular steatosis at histopathologic examination (r = 0.66, P < .001). Correlation between CT and histopathologic examination was poor (r = −0.55, P < .001). A strong correlation was found between T1-weighted dual-echo MR imaging and histopathologic examination (r = 0.85, P < .001) and between ^{1}H MR spectroscopy and histopathologic examination (r = 0.86, P < .001).

In the 23 patients with macrovesicular steatosis greater than 5%, T1-weighted dual-echo MR imaging and ^{1}H MR spectroscopy showed even stronger correlation with histopathologic examination (r = 0.92, P < .001 and r = 0.89, P < .001, respectively) than in the overall group. Also, US and CT showed slightly stronger correlation (r = 0.73, P < .001 and r = −0.64, P = .001, respectively) in patients with hepatic macrovesicular steatosis greater than 5%.

Comparison of Imaging and Spectroscopic Values across Steatosis Grades

Figure 3 shows the performance of CT, T1-weighted dual-echo MR imaging, and ^{1}H MR spectroscopy in differentiating the grades of steatosis. CT could only differentiate between moderate and severe (P < .001) steatosis. T1-weighted dual-echo MR imaging could differentiate between none and mild steatosis (P < .001), between mild and moderate steatosis (P < .001), and between moderate and severe steatosis (P = .04). With ^{1}H MR spectroscopy it was possible to distinguish none from

Figure 1

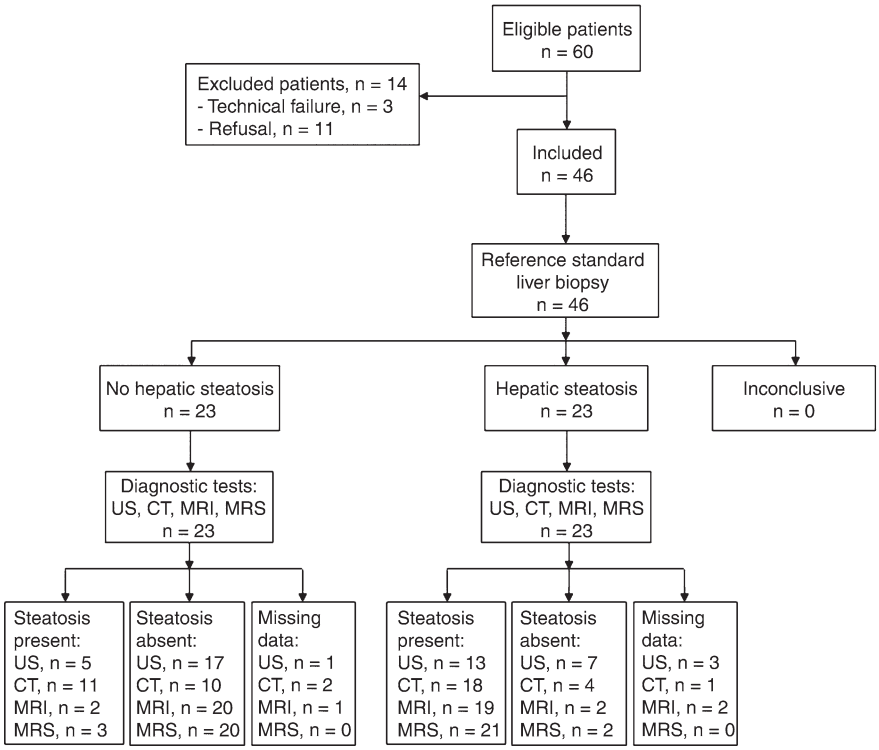

Figure 1: Study flowchart.

mild steatosis ($P < .001$), mild from moderate steatosis ($P < .001$), and moderate from severe steatosis ($P = .01$).

Diagnostic Accuracy

For the 5% upper normal limit histopathologic macrovesicular steatosis threshold value, the diagnostic performance was calculated for the different imaging modalities as summarized in Table 3. We performed ROC curve fitting for US, CT, T1-weighted dual-echo MR imaging, and ^{1}H MR spectroscopy (Fig 4). The AUC was 0.77 for US, 0.76 for CT, 0.93 for T1-weighted dual-echo MR imaging, and 0.97 for ^{1}H MR spectroscopy, showing acceptable diagnostic performance for both T1-weighted dual-echo MR imaging and ^{1}H MR spectroscopy.

From the ROC curves, we found liver attenuation of 54.2 HU as a cut-off value for CT. T1-weighted dual-echo MR imaging hepatic fat fraction had a cut-off value of 1.5% and ^{1}H MR spectroscopy had 1 a cut-off value of 1.8%. For US no cut-off value was calculated (categoric data; steatosis is either present or not). These cut-off values were used to calculate diagnostic accuracy. Lowest sensitivity was found for US (65%, 13 of 20). T1-weighted dual-echo MR imaging and ^{1}H MR spectroscopy had a sensitivity of 90% (19 of 21) and 91% (21 of 23), respectively. Specificity was lowest for CT (70%, 17 of 23) and highest for T1-weighted dual-echo MR imaging (91%, 20 of 22). Positive predictive value and negative predictive value were highest for T1-weighted dual-echo MR imaging (90%, 19 of 21, and 91%, 20 of 22, respectively) and for ^{1}H MR spectroscopy (88%, 21 of 24, and 91%, 20 of 22, respectively). The total accuracy was 71% (30 of 42) for US, 74% (31 of 43) for CT, 91% (39 of 43) for T1-weighted dual-echo MR imaging, and 89% (41 of 46) for ^{1}H MR spectroscopy. The sensitivity of US was significantly lower than that of T1-weighted dual-echo MR imaging ($P = .002$) and ^{1}H MR spectroscopy ($P = .005$); specificity was not different ($P = .664$ and $P = .414$, respectively). The sensitivity of CT was significantly lower than that of T1-weighted dual-echo MR imaging ($P = .039$) and ^{1}H MR spectroscopy ($P = .022$); specificity was not different ($P = .687$ and $P > .99$, respectively). Differences in sensitivity and specificity between T1-weighted dual-echo MR imaging and ^{1}H MR spectroscopy were not significant ($P > .99$). Best positive and negative likelihood ratios were found for T1-weighted dual-echo MR imaging (10.0 and 0.10, respectively) and ^{1}H MR spectroscopy (7.00 and 0.10, respectively).

Finally, by using both CT and T1-weighted dual-echo MR imaging, we found no significant differences in sensitivity (CT and MR imaging, $P > .99$) and specificity (CT, $P > .99$; MR imaging, $P = .625$) in the detection of hepatic fat between the left and right hepatic lobe. Within the right hepatic lobe, we found no significant geographic differences in sensitivity (CT and MR imaging, $P > .99$) and specificity (CT, $P = .787$; MR imaging, $P = .695$) in the detection of hepatic fat.

Discussion

Our study evaluates fully paired measurements of four different hepatic steatosis imaging techniques with histopathologic confirmation. The results demonstrate that both T1-weighted dual-echo MR imaging and ^{1}H MR spectroscopy show stronger correlation with the reference standard and yield higher diagnostic accuracy than do US and CT. Both dual-echo T1-weighted MR imaging and ^{1}H MR spectroscopy allow assessment of steatosis in an objective way, with good sensitivity and specificity.

On the basis of a histopathologic upper limit of 5% macrovesicular steatosis, we calculated a cut-off value of 1.5% for T1-weighted dual-echo MR imaging and of 1.8% for ^{1}H MR spectroscopy. This is significantly lower compared with the population-based cut-off value of 5.6% for ^{1}H MR spectroscopy proposed by Szczepaniak et al (17). Importantly, no histopathologic validation was performed in the latter study. Although

Radiology

Figure 2

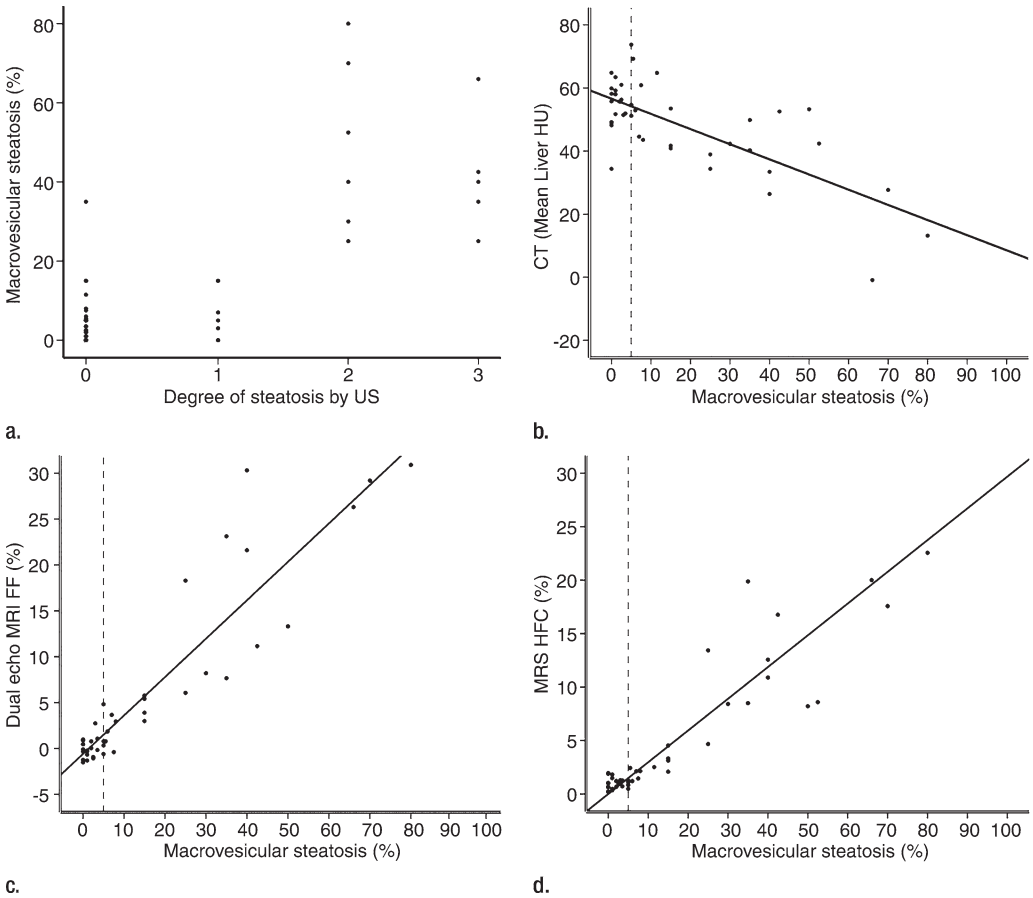

Figure 2: Scatterplots (regression lines in **b–d**) represent correlation between histopathologic results (percentage macrovesicular steatosis) and **(a)** degree of steatosis at US, **(b)** CT liver attenuation, **(c)** T1-weighted dual-echo MR imaging fat fraction *(FF)*, and **(d)** ^{1}H MR spectroscopy hepatic fat content *(HFC)*. Dotted lines represent 5% macrovesicular steatosis cut-off value.

Table 2

Spearman Correlation Coefficients between Imaging Modalities and Histopathologic Examination

	US		CT		MR Imaging		^{1}H MR Spectroscopy	
Patients	*r* Value	*P* Value	*r* Value	*P* Value	*r* Value	*P* Value	*r* Value	*P* Value
All ($n = 46$)	0.66	<.001	−0.55	<.001	0.85	<.001	0.86	<.001
With macrovesicular steatosis greater than 5% ($n = 23$)	0.73	<.001	−0.64	.001	0.92	<.001	0.89	<.001

this upper limit was determined in a sizeable cohort study, the difference in our study is substantial. In a healthy subgroup of this population, hepatic fat showed a median of 1.9% (95th percentile being 5.6%). This much more resembles our calculated upper normal limit of 1.8% hepatic fat.

CT is less suitable for the quantitative assessment of hepatic steatosis. Sensitivity, specificity, and likelihood ratios show insufficient diagnostic performance. This finding is consistent with the results of Park et al (14), who report that it is not clinically acceptable to use CT for the quantitative assessment of steatosis. Although we found acceptable correlation with histopathologic analysis, US also showed poor diagnostic performance. The main disadvantages of US are the inherent subjectivity of the technique, the lack of specificity, the inability to quantify the degree of steatosis, and the limited

Radiology

Figure 3

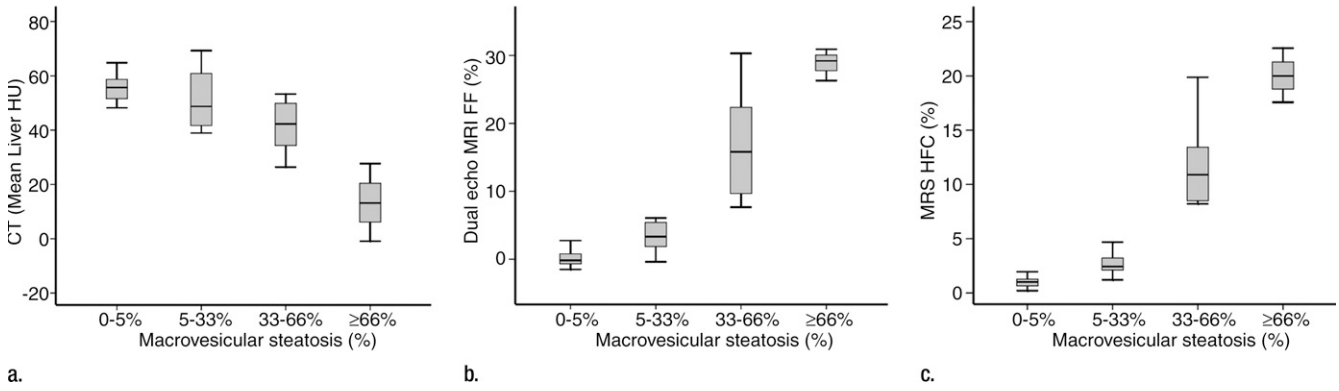

Figure 3: Boxplots represent differences across steatosis grades by using **(a)** CT liver attenuation, **(b)** T1-weighted dual-echo MR imaging fat fraction *(FF)*, and **(c)** single-voxel ^{1}H MR spectroscopy hepatic fat content *(HFC)* in differentiating four stages of hepatic steatosis.

Table 3

Diagnostic Accuracy of US, CT, MR imaging, and ^{1}H MR Spectroscopy for Macrovesicular Hepatic Fat Content

Modality	Sensitivity (%)	Specificity (%)	Positive Predictive Value (%)	Negative Predictive Value (%)	Positive Likelihood Ratio	Negative Likelihood Ratio
US	65 (0.41, 0.84)	77 (0.54, 0.91)	72 (0.46, 0.89)	71 (0.49, 0.87)	2.86	0.45
CT	74 (0.51, 0.89)	70 (0.46, 0.87)	74 (0.51, 0.89)	70 (0.46, 0.87)	2.46	0.37
MR imaging	90 (0.68, 0.98)	91 (0.69, 0.98)	90 (0.68, 0.98)	91 (0.69, 0.98)	10.00	0.10
^{1}H MR spectroscopy	91 (0.70, 0.98)	87 (0.65, 0.97)	88 (0.67, 0.97)	91 (0.69, 0.98)	7.00	0.10

Note.—Data in parentheses are 95% confidence intervals.

range of grading scores of hepatic fat content that can be obtained reliably (low or high hepatic fat content) (37). Furthermore intra- and interobserver variability is substantial (38).

Our study results show that T1-weighted dual-echo MR imaging and ^{1}H MR spectroscopy can both demonstrate differences between clinically relevant grades of macrovesicular steatosis (none, mild, moderate, and severe). This could potentially be relevant for monitoring treatment response in patients with steatosis and in assessing the severity of steatosis in patients undergoing liver resection. With this perspective; ^{1}H MR spectroscopy has already shown to be repeatable and reproducible (18). Furthermore, in living donor liver transplantation procedures, moderate and severe macrovesicular steatosis are considered exclusion criteria (39,40).

Our study had some limitations. We included a relatively small sample size of 46 patients, with only three patients with severe steatosis. Standardization and lifestyle control of patients were not implemented in this study. Since this was not a main objective of our study, we did not study the effect of intra- and interobserver variability on diagnostic performance of the different imaging modalities and histopathologic results.

The performance of CT in our study was relatively poor compared with that in prior studies. There a two important reasons for this. First, other studies have investigated the performance of CT to detect liver steatosis in patients with macrovesicular steatosis greater than 30% (14,41,42). Our study investigated the performance of CT in the entire spectrum of macrovesicular steatosis, thus including the part of the spectrum with poorer CT results. The second reason could be the increased time interval between CT and surgery (and therefore histopathologic analysis) in some patients. Some patients already had unenhanced CT scans from prior diagnostic investigations. When no prior CT scans were available, we performed an unenhanced CT examination 2–3 days before surgery. The redefined maximum time interval between CT and surgery in patients who already had an unenhanced CT scan was 3 months.

Several CT metrics have been studied in recent literature (liver/spleen attenuation index, liver minus spleen attenuation index, and liver attenuation only). Results of different CT metrics used to measure hepatic fat vary in the literature. We chose to investigate liver attenuation only. This metric is advocated by Kodama et al (31). The authors conclude that liver attenuation alone is the best method for predicting hepatic fat content. The attenuation measurement of the spleen does not contribute to the prediction of hepatic fat content. Comparisons of different metrics show that there is no normalization effect with the inclusion of the

Figure 4

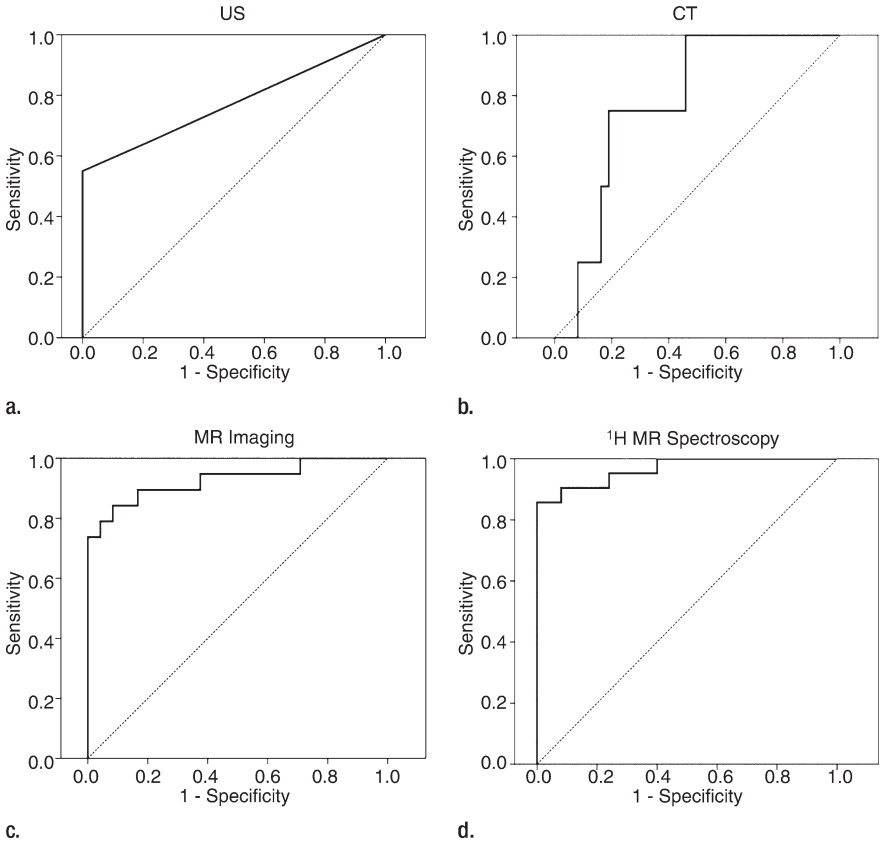

Figure 4: ROC curves represent diagnostic accuracy of **(a)** US, **(b)** CT liver attenuation, **(c)**, T1-weighted dual-echo MR imaging fat fraction, and **(d)** and single-voxel ^{1}H MR spectroscopy in diagnosing hepatic steatosis.

splenic measurements. Comparison of liver attenuation with splenic attenuation is a more complex and time-consuming method than liver attenuation alone.

We used a T1-weighted dual-echo chemical shift MR imaging method for in- and opposed-phase images to study hepatic steatosis. Other authors have suggested more advanced chemical shift imaging methods using multiple echoes (15,43–45). Because the latter method is not widely available, we chose to use the readily available method of T1-weighted dual-echo chemical shift imaging. No corrections for T1, T2*, or fat spectral complexity were made, and consequently only MR signal intensities were evaluated.

In our study, ^{1}H MR spectroscopy was performed during free breathing. This is a potential limitation because the volume interrogated by ^{1}H MR spectroscopy is blurred in the longitudinal direction by 2–3-cm respiratory excursions of the liver. Furthermore, we used a point-resolved spatially localized spectroscopy sequence, which can be confounded by J-coupling effects. We also corrected for T2 relaxation by using T2 values found in the literature. This ignores the variability in T2 relaxation values between individuals. To assess heterogeneity of hepatic fat, one should ideally perform multiple voxel measurements or spectroscopic imaging of the whole liver. However, this would be time consuming and poses higher demands on the shimming of the volume of interest, making it unpractical in clinical practice. Although this is a limitation, the evaluated liver volume at ^{1}H MR spectroscopy is approximately 400 times larger than the amount of liver tissue evaluated at biopsy.

We performed only hematoxylin-eosin staining of the liver biopsy specimens to evaluate hepatic steatosis. We did not perform separate staining for iron. Fibrosis and inflammation were not analyzed. This could pose a confounding effect on the results of our study since elevated iron, fibrosis, and inflammation may be present in patients with hepatic steatosis. Furthermore, we did not consider the effect of microvesicular steatosis on the diagnostic performance of the imaging techniques. In our opinion this is justified since the reference standard was based on macrovesicular steatosis. Compared with microvesicular steatosis, macrovesicular steatosis is predominant at histologic examination (36). Clinically macrovesicular steatosis is more relevant because it is considered to be a risk factor in liver surgery and transplantation (6,40,46,47), but microvesicular steatosis is not (48–50). Furthermore Kleiner et al (36) found that inter- and intraobserver variability to score the amount of microvesicular steatosis was not significantly better than chance (κ score, 0.37 for intraobserver variability and 0.34 for interobserver variability). Therefore, we chose to use only macrovesicular steatosis for analysis in our study.

Another restriction is that we did not perform the imaging measurements at exactly the same location in the liver that were used for histopathologic assessment. This could affect the results we reported in diagnostic performance. However, our results suggest that potential heterogeneity between lobes has no significant effect on diagnostic performance, and we obtained large-wedge liver biopsy specimens, which provided much more and accurate data than could be obtained from percutaneous subcapsular needle biopsy. Furthermore, performance of every measurement at exactly the same locations in the liver was not feasible since the subjects underwent different surgical procedures for tumors of varying sizes and locations. We also noted that ^{1}H MR spectroscopic measurements in the left liver lobe were very sensitive to motion artifacts

because of breathing excursions and smaller size of the left liver lobe.

In this study T1-weighted dual-echo MR imaging and ^{1}H MR spectroscopy had similar findings. We think T1-weighted dual-echo MR imaging performed well because the mean signal intensity decay of 12 ROIs throughout the liver was measured, as opposed to only one voxel measured in the liver with ^{1}H MR spectroscopy. ^{1}H MR spectroscopy might have performed better if multivoxel ^{1}H MR spectroscopic scanning was implemented. In our opinion, ^{1}H MR spectroscopy is also very suitable in clinical practice. Its accuracy is comparable with that of T1-weighted dual-echo MR imaging, and we noticed that it is not more complicated to process, execute, and calculate the proportion of hepatic fat with ^{1}H MR spectroscopy. Unfortunately, ^{1}H MR spectroscopy still lacks general availability in current clinical practice.

In conclusion, T1-weighted dual-echo MR imaging and ^{1}H MR spectroscopy strongly correlate with histopathologic steatosis assessment and are superior to US and CT. In contrast to US and CT, T1-weighted dual-echo MR imaging and ^{1}H MR spectroscopy are better able to depict differences across steatosis grades. These modalities showed the best diagnostic accuracies. Therefore, we conclude that T1-weighted dual-echo MR imaging and ^{1}H MR point-resolved spectroscopy are more accurate for diagnosis and assessment of liver steatosis than are US and CT examinations in patients undergoing liver resection.

References

1. Angulo P. Nonalcoholic fatty liver disease. N Engl J Med 2002;346(16):1221–1231.
2. Bugianesi E, Leone N, Vanni E, et al. Expanding the natural history of nonalcoholic steatohepatitis: from cryptogenic cirrhosis to hepatocellular carcinoma. Gastroenterology 2002;123(1):134–140.
3. Hamaguchi M, Kojima T, Takeda N, et al. The metabolic syndrome as a predictor of nonalcoholic fatty liver disease. Ann Intern Med 2005;143(10):722–728.
4. Ford ES, Giles WH, Mokdad AH. Increasing prevalence of the metabolic syndrome among U.S. adults. Diabetes Care 2004;27(10):2444–2449.
5. Behrns KE, Tsiotos GG, DeSouza NF, Krishna MK, Ludwig J, Nagorney DM. Hepatic steatosis as a potential risk factor for major hepatic resection. J Gastrointest Surg 1998;2(3):292–298.
6. Veteläinen R, van Vliet A, Gouma DJ, van Gulik TM. Steatosis as a risk factor in liver surgery. Ann Surg 2007;245(1):20–30.
7. Adams LA, Angulo P, Lindor KD. Nonalcoholic fatty liver disease. CMAJ 2005;172(7):899–905.
8. Ratziu V, Charlotte F, Heurtier A, et al. Sampling variability of liver biopsy in nonalcoholic fatty liver disease. Gastroenterology 2005;128(7):1898–1906.
9. Bravo AA, Sheth SG, Chopra S. Liver biopsy. N Engl J Med 2001;344(7):495–500.
10. Ma X, Holalkere NS, Kambadakone R A, Mino-Kenudson M, Hahn PF, Sahani DV. Imaging-based quantification of hepatic fat: methods and clinical applications. RadioGraphics 2009;29(5):1253–1277.
11. de Moura Almeida A, Cotrim HP, Barbosa DB, et al. Fatty liver disease in severe obese patients: diagnostic value of abdominal ultrasound. World J Gastroenterol 2008;14(9):1415–1418.
12. Saadeh S, Younossi ZM, Remer EM, et al. The utility of radiological imaging in nonalcoholic fatty liver disease. Gastroenterology 2002;123(3):745–750.
13. Ryan CK, Johnson LA, Germin BI, Marcos A. One hundred consecutive hepatic biopsies in the workup of living donors for right lobe liver transplantation. Liver Transpl 2002;8(12):1114–1122.
14. Park SH, Kim PN, Kim KW, et al. Macrovesicular hepatic steatosis in living liver donors: use of CT for quantitative and qualitative assessment. Radiology 2006;239(1):105–112.
15. Yokoo T, Bydder M, Hamilton G, et al. Nonalcoholic fatty liver disease: diagnostic and fat-grading accuracy of low-flip-angle multiecho gradient-recalled-echo MR imaging at 1.5 T. Radiology 2009;251(1):67–76.
16. Siegelman ES, Rosen MA. Imaging of hepatic steatosis. Semin Liver Dis 2001;21(1):71–80.
17. Szczepaniak LS, Nurenberg P, Leonard D, et al. Magnetic resonance spectroscopy to measure hepatic triglyceride content: prevalence of hepatic steatosis in the general population. Am J Physiol Endocrinol Metab 2005;288(2):E462–E468.
18. van Werven JR, Hoogduin JM, Nederveen AJ, et al. Reproducibility of 3.0 Tesla magnetic resonance spectroscopy for measuring hepatic fat content. J Magn Reson Imaging 2009;30(2):444–448.
19. Guiu B, Petit J, Loffroy R, et al. Quantification of liver fat content: comparison of triple-echo chemical shift gradient echo imaging and in vivo proton MR spectroscopy. Radiology 2009;250(1):95–102.
20. Machann J, Thamer C, Schnoedt B, et al. Hepatic lipid accumulation in healthy subjects: a comparative study using spectral fat-selective MRI and volume-localized 1H-MR spectroscopy. Magn Reson Med 2006;55(4):913–917.
21. Kawamitsu H, Kaji Y, Ohara T, Sugimura K. Feasibility of quantitative intrahepatic lipid imaging applied to the magnetic resonance dual gradient echo sequence. Magn Reson Med Sci 2003;2(1):47–50.
22. Longo R, Ricci C, Masutti F, et al. Fatty infiltration of the liver: quantification by 1H localized magnetic resonance spectroscopy and comparison with computed tomography. Invest Radiol 1993;28(4):297–302.
23. Qayyum A, Chen DM, Breiman RS, et al. Evaluation of diffuse liver steatosis by ultrasound, computed tomography, and magnetic resonance imaging: which modality is best? Clin Imaging 2009;33(2):110–115.
24. Yoshimitsu K, Kuroda Y, Nakamuta M, et al. Noninvasive estimation of hepatic steatosis using plain CT vs chemical-shift MR imaging: significance for living donors. J Magn Reson Imaging 2008;28(3):678–684.
25. Cowin GJ, Jonsson JR, Bauer JD, et al. Magnetic resonance imaging and spectroscopy for monitoring liver steatosis. J Magn Reson Imaging 2008;28(4):937–945.
26. Fishbein M, Castro F, Cheruku S, et al. Hepatic MRI for fat quantification: its relationship to fat morphology, diagnosis, and ultrasound. J Clin Gastroenterol 2005;39(7):619–625.
27. Ataseven H, Yildirim MH, Yalniz M, Bahcecioglu IH, Celebi S, Ozercan IH. The value of ultrasonography and computerized tomography in estimating the histopathological severity of nonalcoholic steatohepatitis. Acta Gastroenterol Belg 2005;68(2):221–225.
28. Thomsen C, Becker U, Winkler K, Christoffersen P, Jensen M, Henriksen O. Quantification of liver fat using magnetic resonance spectroscopy. Magn Reson Imaging 1994;12(3):487–495.
29. Charatcharoenwitthaya P, Lindor KD. Role of radiologic modalities in the management of non-alcoholic steatohepatitis. Clin Liver Dis 2007;11(1):37–54, viii.

30. Mazhar SM, Shiehmorteza M, Sirlin CB. Noninvasive assessment of hepatic steatosis. Clin Gastroenterol Hepatol 2009;7(2):135–140.

31. Kodama Y, Ng CS, Wu TT, et al. Comparison of CT methods for determining the fat content of the liver. AJR Am J Roentgenol 2007;188(5):1307–1312.

32. Cassidy FH, Yokoo T, Aganovic L, et al. Fatty liver disease: MR imaging techniques for the detection and quantification of liver steatosis. RadioGraphics 2009;29(1):231–260.

33. Abramoff MD, Magelhaes PJ, Ram SJ. Image processing with ImageJ. Biophotonics Int 2004;11:36–42.

34. Naressi A, Couturier C, Devos JM, et al. Java-based graphical user interface for the MRUI quantitation package. MAGMA 2001;12(2-3):141–152.

35. de Bazelaire CM, Duhamel GD, Rofsky NM, Alsop DC. MR imaging relaxation times of abdominal and pelvic tissues measured in vivo at 3.0 T: preliminary results. Radiology 2004;230(3):652–659.

36. Kleiner DE, Brunt EM, Van Natta M, et al. Design and validation of a histological scoring system for nonalcoholic fatty liver disease. Hepatology 2005;41(6):1313–1321.

37. Fabbrini E, Conte C, Magkos F. Methods for assessing intrahepatic fat content and steatosis. Curr Opin Clin Nutr Metab Care 2009;12(5):474–481.

38. Strauss S, Gavish E, Gottlieb P, Katsnelson L. Interobserver and intraobserver variability in the sonographic assessment of fatty liver. AJR Am J Roentgenol 2007;189(6):W320–W323.

39. Chen YS, Cheng YF, De Villa VH, et al. Evaluation of living liver donors. Transplantation 2003;75(3 suppl):S16–S19.

40. Barr ML, Belghiti J, Villamil FG, et al. A report of the Vancouver Forum on the care of the live organ donor: lung, liver, pancreas, and intestine data and medical guidelines. Transplantation 2006;81(10):1373–1385.

41. Lee SW, Park SH, Kim KW, et al. Unenhanced CT for assessment of macrovesicular hepatic steatosis in living liver donors: comparison of visual grading with liver attenuation index. Radiology 2007;244(2):479–485.

42. Limanond P, Raman SS, Lassman C, et al. Macrovesicular hepatic steatosis in living related liver donors: correlation between CT and histologic findings. Radiology 2004;230(1):276–280.

43. Yu H, McKenzie CA, Shimakawa A, et al. Multiecho reconstruction for simultaneous water-fat decomposition and T2* estimation. J Magn Reson Imaging 2007;26(4):1153–1161.

44. Bydder M, Yokoo T, Hamilton G, et al. Relaxation effects in the quantification of fat using gradient echo imaging. Magn Reson Imaging 2008;26(3):347–359.

45. Liu CY, McKenzie CA, Yu H, Brittain JH, Reeder SB. Fat quantification with IDEAL gradient echo imaging: correction of bias from T(1) and noise. Magn Reson Med 2007;58(2):354–364.

46. Zamboni F, Franchello A, David E, et al. Effect of macrovescicular steatosis and other donor and recipient characteristics on the outcome of liver transplantation. Clin Transplant 2001;15(1):53–57.

47. Salizzoni M, Franchello A, Zamboni F, et al. Marginal grafts: finding the correct treatment for fatty livers. Transpl Int 2003;16(7):486–493.

48. Ureña MA, Ruiz-Delgado FC, González EM, et al. Assessing risk of the use of livers with macro and microsteatosis in a liver transplant program. Transplant Proc 1998;30(7):3288–3291.

49. Urena MA, Moreno Gonzalez E, Romero CJ, Ruiz-Delgado FC, Moreno Sanz C. An approach to the rational use of steatotic donor livers in liver transplantation. Hepatogastroenterology 1999;46(26):1164–1173.

50. Fishbein TM, Fiel MI, Emre S, et al. Use of livers with microvesicular fat safely expands the donor pool. Transplantation 1997;64(2):248–251.